

Cold-atom Inertial Sensor without Deadtime

B. Fang, I. Dutta, D. Savoie, B. Venon, C. L. Garrido Alzar, R. Geiger and A. Landragin
 LNE-SYRTE, Observatoire de Paris, PSL Research University, CNRS, Sorbonne Universités
 UPMC Univ. Paris 06, 61 avenue de l'Observatoire, 75014 Paris, France
 Email: bess.fang@obspm.fr

Abstract—We report the operation of a cold-atom inertial sensor in a joint interrogation scheme, where we simultaneously prepare a cold-atom source and operate an atom interferometer in order to eliminate dead times. Noise aliasing and dead times are consequences of the sequential operation which is intrinsic to cold-atom atom interferometers. Both phenomena have deleterious effects on the performance of these sensors. We show that our continuous operation improves the short-term sensitivity of atom interferometers, by demonstrating a record rotation sensitivity of $100 \text{ nrad.s}^{-1}/\sqrt{\text{Hz}}$ in a cold-atom gyroscope of 11 cm^2 Sagnac area. We also demonstrate a rotation stability of 1 nrad.s^{-1} after 10^4 s of integration, improving previous results by an order of magnitude. We expect that the continuous operation will allow cold-atom inertial sensors with long interrogation time to reach their full sensitivity, determined by the quantum noise limit.

I. INTRODUCTION

Over the last twenty years, inertial sensors based on atom interferometry have evolved significantly in terms of performance and transportability. Such progress ensures the relevance of atom interferometer (AI) based inertial sensors in various field applications, ranging from inertial navigation [1], [2], [3] to geophysics and geodesy [4], [5], [6], [7], as well as in fundamental physics [8], [9], [10]. Although new techniques are currently explored to further improve the sensitivity of these sensors [11], [12], [13], [14], [15], the issues associated with measurement dead time remain a strong obstacle to their ultimate performance [16].

Dead times in AIs correspond to the time needed to prepare and to detect the atoms before and after the interferometric sequence. They result in loss of inertial information, leaving AIs unsuitable for inertial measurement units (IMUs) in navigation [17] or for recording fast varying signals in seismology [18] for the time being. Noise aliasing coming from the sequential operation also degrades the AI sensitivity in the presence of dead times, similar to the Dick effect in cold atomic clocks [19].

In this paper, we report the first continuous operation of a cold-atom inertial sensor. This is demonstrated in a gyroscope configuration featuring a macroscopic Sagnac area of 11 cm^2 . We achieve a short-term rotation stability of $100 \text{ nrad.s}^{-1}/\sqrt{\text{Hz}}$, and a long-term stability as low as 1 nrad.s^{-1} after 10^4 s of integration, setting the record of all atom gyroscopes.

II. EXPERIMENTAL SETUP

We realize a light-pulse gyroscope in a cesium fountain, see Fig. 1. Counter-propagating Raman beams coupling the

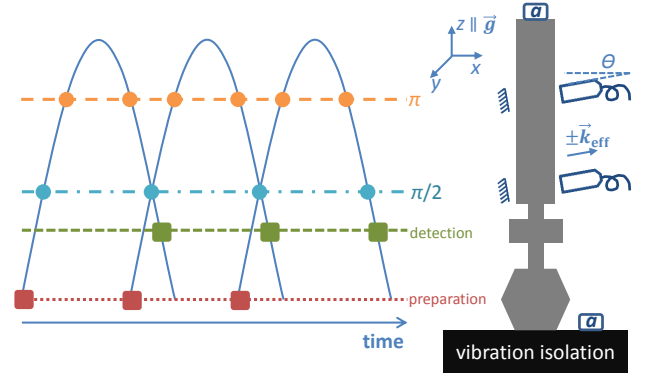


Fig. 1. Operation principle and setup of the continuous cold-atom gyroscope.

$|F = 4, m_F = 0\rangle$ and $|F = 3, m_F = 0\rangle$ clock states are used to split, deflect and recombine the free-falling cold atoms¹. With four light pulses ($\pi/2$ - π - π - $\pi/2$), the two arms of the interferometer enclose a physical area up to 11 cm^2 , representing a 27-fold increase with respect to previous experiments [21]. This gives rise to a rotation phase shift Φ_Ω according to the Sagnac effect [22], given by

$$\Phi_\Omega = \frac{1}{2} \vec{k}_{\text{eff}} \cdot \left(\vec{g} \times \vec{\Omega} \right) T^3, \quad (1)$$

where \vec{k}_{eff} is the two-photon momentum transfer, \vec{g} is the gravitational acceleration, $\vec{\Omega}$ is the rotation rate, and T is half the interferometric time. Following the atom juggling methods initially introduced to measure collisional shifts in fountain clocks [23], we implement a sequence of joint interrogation of successive atom clouds as described in [24]. In other words, each $\pi/2$ Raman pulse is common to the two adjacent interferometer sequences, setting the cycle time T_c equal to the total interrogation time $2T$.

The interrogation light contains two frequencies, each addressing one of the two clock states. The counter-propagating configuration is achieved by means of retroreflecting the incoming beam (see Fig. 1), so that two configurations are possible, transferring opposite momenta (denoted as $\pm \vec{k}_{\text{eff}}$) to the atoms. The degeneracy of these two configurations is lifted by tilting the Raman beams by an angle of inclination $\theta \simeq 4^\circ$, as the Doppler effect associated with the vertical velocity of the atoms shifts the resonance frequency of the

¹We focus on the inertial measurement and analysis in this paper. Details of the atom preparation and detection can be found in [20].

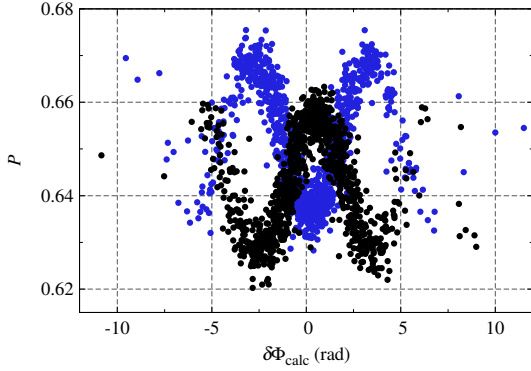


Fig. 2. Measured probability P versus calculated vibration phase $\delta\Phi_{\text{calc}}$ for the $\pm\vec{k}_{\text{eff}}$ configurations.

stimulated Raman transition in the opposite directions. The joint interrogation simultaneously addresses two atom clouds with opposite vertical velocity, thus alternating between the $\pm\vec{k}_{\text{eff}}$ configurations.

Increasing the sensitivity of such AI-based inertial sensors necessarily comes at the cost of an increased sensitivity to the vibration noise, as a consequence of the Equivalence Principle. Noninertial effects such as the Raman laser phase noise and light shift also contribute to the interferometer output. We can thus breakdown the interferometric phase into rotation phase, vibration phase and noninertial phase, i.e. $\Delta\Phi = \Phi_{\Omega} + \delta\Phi_{\text{vib}} + \delta\Phi_0$. Vibration noise has a strong impact on our setup. A vibration isolation platform reduces the effect of the ground vibration $\gtrsim 1$ Hz to an rms AI phase noise of about 2.5 rad for $2T = 800$ ms. Since the vibration noise spans several interferometer fringes, auxiliary inertial sensors are necessary to recover the signal.

We use two commercial accelerometers (marked ‘a’ in Fig. 1) to record and correct the vibration noise. The acquired acceleration signal is weighted using the transfer function [25] in order to compute the vibration phase. Fig. 2 shows the measured probability of transition P versus the calculated vibration phase $\delta\Phi_{\text{calc}}$ for the $\pm\vec{k}_{\text{eff}}$ configurations. Despite the overwhelmingly large vibration noise, the inertial stability of our gyroscope is given by the horizontal scatter of the fringes. This will be evaluated in the following section.

III. STABILITY OF ROTATION MEASUREMENT

We divide a data set into packets of 40 points. As the data alternates between the the $\pm\vec{k}_{\text{eff}}$ configurations, 20 points of each configuration are used to fit a sinusoidal model,

$$P = P_0 + A \cos(\delta\Phi_{\text{calc}} + \Phi^{(\pm)}), \quad (2)$$

where P_0 is the offset of the interferometric signal, A is the fringe amplitude, and the phase offset is given by $\Phi^{(\pm)} = \pm\Phi_{\Omega} + \delta\Phi_0$. This yields a rotation phase $\Phi_{\Omega} \equiv (\Phi^{(+)} - \Phi^{(-)})/2 \pmod{\pi}$. All fitting parameters P_0 , A and $\Phi^{(\pm)}$ were constrained loosely in order to avoid cross talk between phase noise and probability or amplitude noise. The convergence of

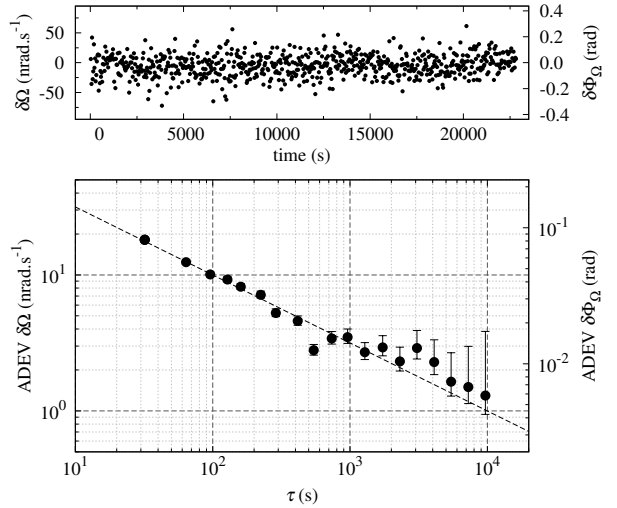


Fig. 3. Top: The time sequence of rotation rate measurement around its mean value. The equivalent fluctuation of rotation phase is shown on the right axis. Bottom: ADEV of the measurement. The error bars indicate the 68% confidence interval, and the dashed line follows a $\tau^{-1/2}$ scaling.

the fit routine is ensured by the large span of the vibration phase.

Figure 3 (top) shows an uninterrupted measurement over about 6 hours. The Allan standard deviation (ADEV) of the rotation rate sensitivity is shown in Fig. 3 (bottom). As the ADEV follows the $\tau^{-1/2}$ scaling, where τ is the integration time, we obtain a short-term rotation sensitivity of $100 \text{ nrad.s}^{-1}/\sqrt{\text{Hz}}$. This establishes the best performance among all cold-atom gyroscopes to date [21], and represents a 30-fold improvement compared to previous four-pulse gyroscopes [1], [3]. Comparing the normal and the continuous mode, the performance of our gyroscope improves by about a factor 1.4. This is consistent with the speedup of the cycling frequency ².

Such a sensitivity is currently limited by the detection noise (about $400 \text{ mrad}/\sqrt{\text{Hz}}$ for $A \simeq 2\%$). This also bounds the efficiency of the vibration correction protocol to about a factor 5 in the present case. The technical difficulties associated with the joint operation (primarily light shift and contrast reduction due to scattered light by the MOT) are assessed in [24], together with strategies for improvement.

Nevertheless, the long-term stability of our rotation rate measurement reaches 1 nrad.s^{-1} after 10^4 s of integration time. This represents the state of the art of all atom gyroscopes [26] (see [27] for a recent review), and a 20-fold improvement from previous cold-atom gyroscopes [21], [28]. Such a stability is a direct consequence of the macroscopic Sagnac area and the folded four-pulse geometry, giving a T^3 dependence of the scale factor. With a long interrogation time, fluctuations of the atom cloud trajectories, a known limit in previous experiments [21], [28], are scaled down for its linear

²The dead time in normal mode $T_D = 0.8$ s by coincidence, so that the cycling frequency doubles when we operate our gyroscope in the continuous mode.

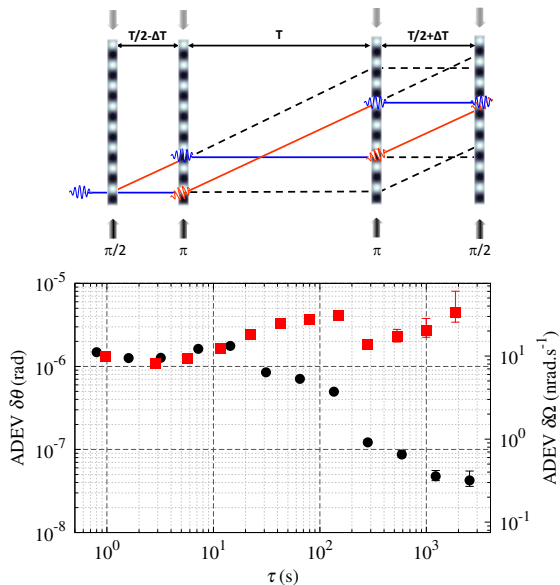


Fig. 4. Top: The space-time diagram of the asymmetric four-pulse interferometer. Bottom: ADEV of the tilt measurement before (squares) and after (circles) active stabilization.

dependence in T . One-photon light shift, a source of slow drift in stability due to the drift of the power ratio of the Raman lasers, is removed by combining the measurement from the $\pm \vec{k}_{\text{eff}}$ configurations.

A symmetric four-pulse interferometer offers zero sensitivity to a DC acceleration parallel to \vec{k}_{eff} . This however comes at the expense of an enhanced probability noise in practice, as imperfect π pulses give rise to parasitic interferometers [3]. We introduce a timing asymmetry of $\Delta T = 300 \mu\text{s}$, see Fig. 4 (top), in order to prevent the closure of the parasitic interferometers. This gives rise to a sensitivity to DC accelerations, $\Phi_{\text{DC}} = 2k_{\text{eff}}T\Delta Tg \sin \theta$. In other words, a 1 mrad fluctuation of θ translates into a ~ 70 rad fluctuation of Φ_{DC} . We therefore stabilize the tilt of the experiment to reduce these fluctuations. A commercial tiltmeter is used to acquire the tilt signal, the variations of which are compensated by a current controlled magnetic actuator acting on the vibration platform. Figure 4 (bottom) shows the ADEV of $\delta\theta$ with and without the tilt lock. We stabilize $\delta\theta$ down to $\sim 4 \times 10^{-8}$ rad, corresponding to a long-term stabilization of Φ_{DC} below 0.3 nrad.s^{-1} level after 2000 s of integration. Alternating measurements between $\Delta T = \pm 300 \mu\text{s}$ allowed us to verify that Φ_{DC} does not impact the stability of the rotation rate measurement. We also monitor the cross-axis tilt and observe a negligible phase drift due to the change of the projection of the rotation vector on the interferometer area.

IV. TOWARDS QUANTUM NOISE LIMITED ATOM INTERFEROMETERS

The continuous operation introduces phase correlations between successive measurements. This in principle allows faster noise averaging following a τ^{-1} scaling in ADEV. It has been demonstrated on our setup in the clock mode [24] where the

Dick effect from a degraded local oscillator is quickly reduced with integration.

In order to demonstrate the same τ^{-1} scaling in our inertial measurements, we need to reduce the uncorrelated detection noise, and to operate our AI at mid-fringe in order to preserve the maximal sensitivity, i.e. $|dP/d\Delta\Phi| = A$. This is confirmed by a simulation of the ADEV for different levels of vibration noise, which is corrected by auxiliary sensors. The residual phase noise $\delta\Phi_{\text{res}}$ (including the inertial noise not corrected by the auxiliary sensors and some noninertial noise) is correlated between successive shots. Its rms $\sigma_{\text{res}} = 120$ mrad is kept constant in all three cases. The vibration noise calculated from the auxiliary sensor signals is generated randomly, with an rms of $\sigma_{\text{calc}} = 0.13$ rad, 0.32 rad, and 2.1 rad. For $P_0 = 0.5$ and $A = 5\%$, we compute $P = P_0 - A \sin(\delta\Phi_{\text{calc}} + \delta\Phi_{\text{res}})$ to simulate the AI operation. Fitting P versus $\delta\Phi_{\text{calc}}$ using 10-point packets yields $\delta\Phi_{\text{res}}^{(\text{fit})}$, similar to our data analysis procedure. The ADEV of $\delta\Phi_{\text{res}}^{(\text{fit})}$ is shown in Fig. 5, indicating a loss of the τ^{-1} scaling when the vibration noise brings the AI out of the linear regime. Note that fringe fitting is equivalent to linear regression as long as the AI remains at mid-fringe, see Fig. 5 (a).

We can retain a mid-fringe operation using a real-time compensation of the vibration noise, first demonstrated on an atom gravimeter [29]. A phase jump of the interrogation laser right before the end of the interferometer sequence can cancel the vibration phase and reduce the span of the interferometric phase. Alternatively, we can implement a more elaborated protocol using quantum weak measurement, as shown in the clock mode in [30]. Assuming a quantum projection noise limited detection with 10^6 atoms and $A = 10\%$, a rotation sensitivity below $1 \times 10^{-10} \text{ rad.s}^{-1}$ in a few 100 s is accessible with our setup.

V. CONCLUSION

The continuous operation of our atom gyroscope allows us to improve the stability of the rotation rate measurement without loss of inertial information. We report $100 \text{ nrad.s}^{-1}/\sqrt{\text{Hz}}$ rotation sensitivity, and a stability of 1 nrad.s^{-1} after 10^4 s of integration. This is well within the specifications of a strategic grade gyroscope ($< 4 \text{ nrad.s}^{-1}$ stability [31]), making AI more attractive for inertial navigation. We also foresee applications in geodesy and geophysics, where seismic signals in the a few mHz to 10s of Hz frequency band could be accessible with such inertial sensors. AI operating in continuous mode are also useful in the search of time-dependent signals such as gravitational waves [9], [10].

ACKNOWLEDGEMENT

We acknowledge the financial support from Délégation Générale de l'Armement (contract No. 2010.34.0005), Centre National d'Etudes Saptiales, Institut Francilien de Recherche sur les Atomes Froids, the Action Spécifique du CNRS Gravitation, Références, Astronomie et Métrologie and Ville de Paris (project HSENS-MWGRAV). I.D. was supported by

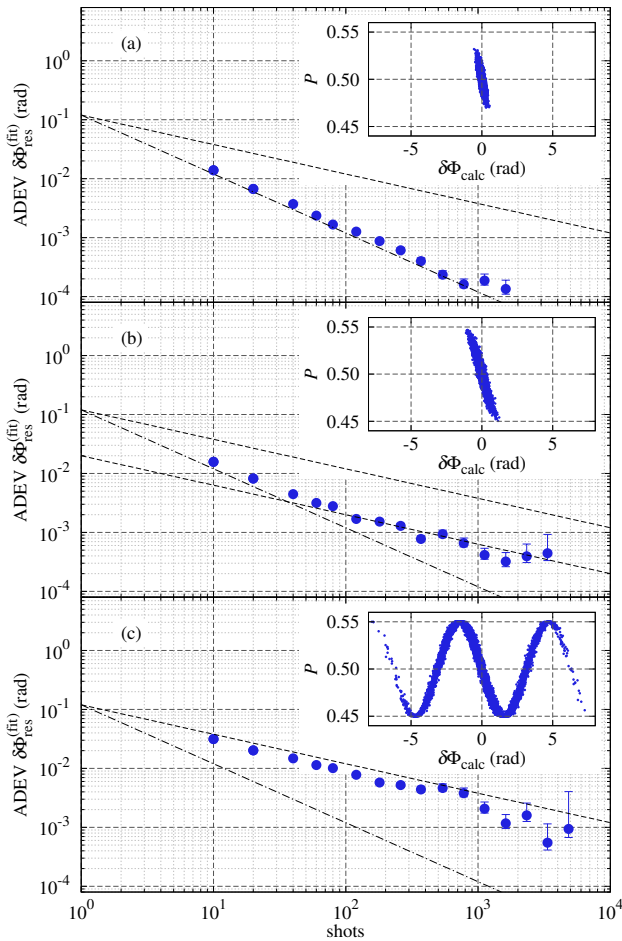


Fig. 5. Simulation of the gyroscope phase stability with increasing vibration noise. (a) - (c) correspond to $\sigma_{\text{vib}} = 0.13$ rad, 0.32 rad, and 2.1 rad added to a constant level of residual correlated noise $\sigma_{\text{res}} = 120$ mrad. The fast noise averaging following τ^{-1} scaling (dash-dotted lines) is gradually lost for AIs that operate away from mid-fringe, recovering the $\tau^{-1/2}$ scaling (dashed lines). The insets show the simulated P versus $\delta\Phi_{\text{calc}}$.

CNES and FIRST-TF (ANR-10-LABX-48-01), D.S. by DGA and B.F. by FIRST-TF.

REFERENCES

- [1] B. Canuel, F. Leduc, D. Holleville, A. Gauguier, J. Fils, A. Virdis, A. Clairon, N. Dimarcq, C. J. Bordé, A. Landragin, and P. Bouyer, "Six-axis inertial sensor using cold-atom interferometry," *Phys. Rev. Lett.*, vol. 97, p. 010402, Jul 2006.
- [2] R. Geiger, V. Menoret, G. Stern, N. Zahzam, P. Cheinet, B. Battelier, A. Villing, F. Moron, M. Lours, Y. Bidel, A. Bresson, A. Landragin, and P. Bouyer, "Detecting inertial effects with airborne matter-wave interferometry," *Nat Commun*, vol. 2, p. 474, Sep. 2011.
- [3] J. K. Stockton, K. Takase, and M. A. Kasevich, "Absolute Geodetic Rotation Measurement Using Atom Interferometry," *Phys. Rev. Lett.*, vol. 107, no. 13, p. 133001, Sep. 2011.
- [4] P. Gillot, O. Francis, A. Landragin, F. P. D. Santos, and S. Merlet, "Stability comparison of two absolute gravimeters: optical versus atomic interferometers," *Metrologia*, vol. 51, no. 5, p. L15, 2014.
- [5] R. Geiger et al, "Matter-wave laser interferometric gravitation antenna (miga): New perspectives for fundamental physics and geosciences," in *Proceedings of the 50th Rencontres de Moriond*, 2015.
- [6] C. Freier, M. Hauth, V. Schkolnik, B. Leykauf, M. Schilling, H. Wziontek, H.-G. Scherneck, J. Müller, and A. Peters, "Mobile quantum

- gravity sensor with unprecedented stability," in *Proceedings for the 8th Symposium on Frequency Standards and Metrology*, 2015.
- [7] G. Rosi, L. Cacciapuoti, F. Sorrentino, M. Menchetti, M. Prevedelli, and G. M. Tino, "Measurement of the gravity-field curvature by atom interferometry," *Phys. Rev. Lett.*, vol. 114, p. 013001, Jan 2015.
- [8] B. Altschul, Q. G. Bailey, L. Blanchet, K. Bongs, P. Bouyer, L. Cacciapuoti, S. Capozziello, N. Gaaloul, D. Giulini, J. Hartwig, L. Iessm, P. Jetzer, A. Landragin, E. Rasel, S. Reynaud, S. Schiller, C. Schubert, F. Sorrentino, U. Sterr, J. D. Tasson, G. M. Tino, P. Tuckey, and P. Wolf, "Quantum tests of the einstein equivalence principle with the ste?quest space mission," *Advances in Space Research*, vol. 50, p. 501, 2015.
- [9] S. Dimopoulos, P. W. Graham, J. M. Hogan, M. A. Kasevich, and S. Rajendran, "Atomic gravitational wave interferometric sensor," *Phys. Rev. D*, vol. 78, p. 122002, Dec 2008.
- [10] W. Chaibi, R. Geiger, B. Canuel, A. Bertoldi, A. Landragin, and P. Bouyer, "Low frequency gravitational wave detection with ground-based atom interferometer arrays," *Phys. Rev. D*, vol. 93, p. 021101, Jan 2016.
- [11] P. Cladé, S. Guellati-Khélifa, F. Nez, and F. Biraben, "Large momentum beam splitter using bloch oscillations," *Phys. Rev. Lett.*, vol. 102, p. 240402, Jun 2009.
- [12] S.-w. Chiow, T. Kovachy, H.-C. Chien, and M. A. Kasevich, "102hk large area atom interferometers," *Phys. Rev. Lett.*, vol. 107, p. 130403, Sep 2011.
- [13] J. E. Debs, P. A. Altin, T. H. Barter, D. Döring, G. R. Dennis, G. McDonald, R. P. Anderson, J. D. Close, and N. P. Robins, "Cold-atom gravimetry with a bose-einstein condensate," *Phys. Rev. A*, vol. 84, p. 033610, Sep 2011.
- [14] I. D. Leroux, M. H. Schleier-Smith, and V. Vuletić, "Implementation of cavity squeezing of a collective atomic spin," *Phys. Rev. Lett.*, vol. 104, p. 073602, Feb 2010.
- [15] O. Hosten, N. J. Engelsen, R. Krishnakumar, and M. A. Kasevich, "Measurement noise 100 times lower than the quantum-projection limit using entangled atoms," *Nature*, vol. 529, no. 7587, pp. 505–508, Jan. 2016.
- [16] B. Fang, I. Dutta, P. Gillot, D. Savoie, J. Lautier, B. Cheng, C. L. Garrido Alzar, R. Geiger, S. Merlet, F. Pereira Dos Santos, and A. Landragin, "Metrology with atom interferometry: Inertial sensors from laboratory to field applications," in *Proceedings for the 8th Symposium on Frequency Standards and Metrology*, 2016.
- [17] C. Jekeli, "Navigation Error Analysis of Atom Interferometer Inertial Sensor," *Navigation*, vol. 52, no. 1, pp. 1–14, Mar. 2005.
- [18] K. U. Schreiber and J.-P. R. Wells, "Invited review article: Large ring lasers for rotation sensing," *Rev. Sci. Instrum.*, vol. 84, no. 4, 2013.
- [19] G. Santarelli, A. Audoin, C. and Makdissi, P. Laurent, G. J. Dick, and A. Clairon, "Frequency stability degradation of an oscillator slaved to a periodically interrogated atomic resonator," *IEEE Trans. Ultrason. Ferroelectr. Freq. Control*, vol. 45, pp. 887–894, 1998.
- [20] I. Dutta, D. Savoie, B. Fang, B. Venon, C. L. Garrido Alzar, R. Geiger, and A. Landragin, "Continuous cold-atom inertial sensor with 1 nrad.s⁻¹ rotation stability," *Phys. Rev. Lett.*, vol. 116, p. 183003, 2016.
- [21] P. Berg, S. Abend, G. Tackmann, C. Schubert, E. Giese, W. P. Schleich, F. A. Narducci, W. Ertmer, and E. M. Rasel, "Composite-Light-Pulse Technique for High-Precision Atom Interferometry," *Phys. Rev. Lett.*, vol. 114, no. 6, p. 063002, Feb. 2015.
- [22] G. Sagnac, "L'éther lumineux démontré par l'effet du vent relatif d'éther dans un interféromètre en rotation uniforme," *C. R. Acad. Sci. (Paris)*, vol. 157, p. 708, 1913.
- [23] R. Legere and K. Gibble, "Quantum scattering in a juggling atomic fountain," *Phys. Rev. Lett.*, vol. 81, pp. 5780–5783, Dec 1998.
- [24] M. Meunier, I. Dutta, R. Geiger, C. Guerlin, C. L. Garrido Alzar, and A. Landragin, "Stability enhancement by joint phase measurements in a single cold atomic fountain," *Phys. Rev. A*, vol. 90, p. 063633, Dec 2014.
- [25] P. Cheinet, B. Canuel, F. Pereira Dos Santos, A. Gauguier, F. Leduc, and A. Landragin, "Measurement of the sensitivity function in time-domain atomic interferometer," *IEEE Trans. on Instrum. Meas.*, vol. 57, p. 1141, 2008.
- [26] D. S. Durfee, Y. K. Shaham, and M. A. Kasevich, "Long-term stability of an area-reversible atom-interferometer sagnac gyroscope," *Phys. Rev. Lett.*, vol. 97, p. 240801, Dec 2006.
- [27] B. Barrett, R. Geiger, I. Dutta, M. Meunier, B. Canuel, A. Gauguier, P. Bouyer, and A. Landragin, "The Sagnac effect: 20 years of develop-

- ment in matter-wave interferometry,” *Comptes Rendus Physique*, vol. 15, no. 10, pp. 875–883, Dec. 2014.
- [28] A. Gauguet, B. Canuel, T. Lvque, W. Chaibi, and A. Landragin, “Characterization and limits of a cold-atom Sagnac interferometer,” *Phys. Rev. A*, vol. 80, no. 6, p. 063604, Dec. 2009.
- [29] J. Lautier, L. Volodimer, T. Hardin, S. Merlet, M. Lours, F. Pereira Dos Santos, and A. Landragin, “Hybridizing matter-wave and classical accelerometers,” *Appl. Phys. Lett.*, vol. 105, no. 14, p. 144102, Oct. 2014.
- [30] R. Kohlhaas, A. Bertoldi, E. Cantin, A. Aspect, A. Landragin, and P. Bouyer, “Phase locking a clock oscillator to a coherent atomic ensemble,” *Phys. Rev. X*, vol. 5, p. 021011, Apr 2015.
- [31] H. C. Lefèvre, “The fiber-optic gyroscope, a century after Sagnac’s experiment: The ultimate rotation-sensing technology?” *Comptes Rendus Physique*, vol. 15, no. 10, pp. 851–858, Dec. 2014.